G-protein-coupled receptor signaling in a patient with acrodysostosis and hormone resistance. *J Clin Endocrinol Metab* 97 (9): E1808–1813, 2012.
18. Kagami M, Matsuoka K, Nagai T, Yamanaka M, Kurosawa K, Suzumori N, Sekita Y, Miyado M, Matsubara K, Fuke T, Kato F, Fukami M, Ogata T*: Paternal uniparental disomy 14 and related disorders: placental gene expression analyses and histological examinations. *Epigenetics* 7 (10): 1142–1150, 2012.
19. Moritani M, Yokota I, Tsubouchi K, Takaya R, Takemoto K, Minamitani K, Urakami T, Kawamura T, Kikuchi N, Itakura M, Ogata T, Sugihara S, Amemiya S: Identification of INS and KCNJ11 gene mutations in type 1B diabetes in Japanese children with onset of diabetes before 5 yr of age. *Pediatr Diabetes*
20. Suzuki-Suwanai A, Ishii T, Haruna H, Yamataka A, Narumi S, Fukuzawa R, Ogata T, Hasegawa T*: A report of two novel NR5A1 mutation families: possible clinical phenotype of psychiatric symptoms of anxiety and/or depression. *Clin Endocrinol* (accepted).
21. Miyado M, Nakamura M, Miyado K, Morohashi K, Sano S, Nagata E, Fukami M, , Ogata T*: *Mamld1* deficiency significantly reduces mRNA expression levels of multiple genes expressed in mouse fetal Leydig cells but permits normal genital and reproductive development. *Endocrinology* (accepted).
22. Sekii K*, Itoh H, Ogata T, Iwashima S*: Possible contribution of fetal size and gestational age to myocardial tissue Doppler velocities in preterm fetuses. *Eur J Obstet Gynecol Reprod Biol* (accepted).
23. Nagasaki K*, Tsuchuya S, Saitoh A, Ogata T, Fukami M: Neuromuscular symptoms in a patient with familial pseudohypoparathyroidism type Ib diagnosed by methylation-specific multiplex ligation-dependent probe amplification. *Endocr J* (accepted).
24. Ohishi A*, Ueno D, Matsuoka, H, Kawamoto, F Ogata T: Glucose-6-phosphate dehydrogenase deficiency and adrenal hemorrhage in a Filipino neonate with hyperbilirubinemia. *Am J Perinatol Reports* (in press).
25. Fuke T, Mizuno S, Nagai T, Hasegawa T, Horikawa R, Miyoshi Y, Muroya K, Kondoh T, Numakura C, Sato S, Nakabayashi K, Tayama C, Hata K, Sano S, Matsubara K, Kagami M, Tamazawa K, Ogata T*: Molecular and clinical studies in 138 Japanese patients with Silver-Russell syndrome. *PLoS ONE* (accepted).
26. Ayabe T, Matsubara K, Ogata T, Ayabe A, Murakami N, Nagai T, Fukami M*: Birth seasonality in Prader-Willi syndrome resulting from chromosome 15 microdeletion. *Am J Med Genet A* (accepted).
27. Fukami M*, Shozu M, Ogata T: Molecular bases and phenotypic determinants of aromatase excess syndrome. *Int J Endocrinol* 2012: 584807, 2012.
28. Ogata T*, Sano S, Nagata E, kato F, Fumaki M: *MAMLD1* and 46,XY disorders of sex development. *Semi Reprod Med* 30 (5): 410–416, 2012.
29. Fukami M, Homma K, Hasegawa T, Ogata T*: Backdoor pathway for dihydrotestosterone biosynthesis: implications for normal and abnormal human sex development. *Dev Dyn* 2012 Oct 16. doi: 10.1002/dvdy.23892. [Epub ahead of print].

２．学会発表

省略

G. 知的財産権の出願・登録状況

該当なし

研究成果の刊行に関する一覧表

書籍

著者氏名	論文タイトル名	書籍全体の編集者名	書　籍　名	出版社名	出版地	出版年	ページ

雑誌

発表者氏名	論文タイトル名	発表誌名	巻号	ページ	出版年
Inoue H, Mukai T, Sakamoto Y, Ogata T, et al.	Identification of a novel mutation in the exon 2 splice donor site of the POU1F1/PIT-1 gene in Japanese identical twins with mild combined pituitary hormone deficiency.	*Clin Endocrinol*	76 (1)	78–87	2012
Sugihara S*, Ogata T, Kawamura T, Urakami T, et al.	Genetic characteristics on HLA-cass II and class I among Japanese type 1A and type 1B diabetic children and their families.	*Pediatr Diabetes*	13 (1)	33–44	2012
Kagami M, Kato F, Matsubara K, Sato T, Nishimura G, Ogata T*	Relative frequency of underlying genetic causes for the development of UPD(14)pat-like phenotype.	*Eur J Hum Genet*	20 (9)	928–932	2012
Oto Y*, Obata K, Matsubara K, Ogata T,et al.	Growth hormone secretion and its effect on height in pediatric patients with different genotypes of Prader-Willi syndrome.	*Am J Med Genet A*	158A (6)	1477–1480	2012
Fuke-Sato T, Yamazawa K, Nakabayashi K, Ogata T*et al.	Mosaic upd(7)mat in a patient with Silver-Russell syndrome: correlation between phenotype and mosaic ratio in the body and the placenta.	*Am J Med Genet A*	158A (2)	465–468	2012
Stoppa-Vaucher S, Ayabe T, Paquette J, Ogata T, et al.	46, XY gonadal dysgenesis: new *SRY* point mutation in two siblings with paternal germ line mosaicism.	*Clin Genet*	82 (6)	505–513	2012
Abe Y, Aoki Y*, Kuriyama S, Ogata T, et al.	Prevalence and clinical features of Costello syndrome and cardio-facio-cutaneous syndrome in Japan: Findings from a nationwide epidemiological survey.	*Am J Med Genet A*	158A (5)	1083–1094	2012

Koyama Y*, Homma K, Fukami M, Ogata T, et al.	Two-step biochemical differential diagnosis of classical 21-hydroxylase deficiency and cytochrome P450 oxidoreductase deficiency in Japanese infants using uUrinary Pregnanetriolone / Tetrahydroxycortisone Ratio and 11β-hydroxyandrosterone by Gas chromatography - mass spectrometry.	*Clin Chem*	58 (4)	741–747	2012
Sekii K*, Itoh H, Ogata T,et al.	Deterioration of myocardial tissue Doppler indices in a case of fetal hydrothorax as a promising indication for clinical intervention before the development of nonimmune hydrops fetalis.	*Arch Gynecol Obstet*	286 (4)	1079–1080	2012
Kalfa N, Fukami M, Philibert P, Ogata T, et al.	Screening of *MAMLD1* mutations in 70 Children with 46,XY DSD: Identification and functional analysis of two new mutations.	*PLoS One*	7 (3)	e32505	2012
Qin X-Y, Miyado M, Kojima Y, Ogata T, et al	Identification of novel low-dose bisphenol a targets in human foreskin fibroblast cells derived from hypospadias patients.	*PLoS ONE*	7 (5)	e36711	2012
Sekii K*, Ishikawa T, Ogata T, Itoh H, Iwashima S.	Fetal myocardial tissue Doppler indices before birth physiologically change in proportion to body size adjusted for gestational age in low-risk term pregnancies.	*Early Hum Dev*	88 (7)	517–523	2012
Fukami M*, Tsuchiya T, Takada S, Ogata T,et al.	Complex genomic rearrangements in the *SOX9* 5' region in a patient with Pierre Robin sequence and hypoplastic left scapula.	*Am J Med Genet A*	158A (7)	1529–1534	2012
Ogata T*, Fukami M, Yoshida R, Nagata E, Fujisawa Y, Yoshida A, Yoshimura Y	Haplotype analysis of *ESR2* in Japanese patients with spermatogenic failure.	*J Hum Genet*	57 (7)	449–452	2012
Qin X-Y, Kojima Y, Ogata T,et al.	Association of variants in genes involved in environmental chemical metabolism and risk of cryptorchidism and hypospadias	*J Hum Genet*	57 (7)	434–441	2012
Hiura H, Okae H, Miyauchi N, Ogata T, et al.	Characterization of DNA methylation errors in patients with imprinting disorders conceived by assisted reproduction technologies.	*Hum Reprod*	27 (8)	2541–2548	2012
Nagasaki K, Iida T, Ogata T,et al.	*PRKAR1A* mutation affecting cAMP-mediated G-protein-coupled receptor signaling in a patient with acrodysostosis and hormone resistance.	*J Clin Endocrinol Metab*	97 (9)	E1808–1813	2012
Kagami M, Matsuoka K, Nagai T, Ogata T,et al.	Paternal uniparental disomy 14 and related disorders: placental gene expression analyses and histological examinations.	*Epigenetics*	7 (10)	1142–1150	2012
Moritani M, Yokota I, Tsubouchi K, Ogata T,et al.	Identification of INS and KCNJ11 gene mutations in type 1B diabetes in Japanese children with onset of diabetes before 5 yr of age.	*Pediatr Diabetes*	2012 Sep 10. doi	10.1111/j.1399-5448.2012.00917.x.	[Epub ahead of print]
Suzuki-Suwanai A, Ishii T, Haruna H, Ogata T,et al.	A report of two novel NR5A1 mutation families: possible clinical phenotype of psychiatric symptoms of anxiety and/or depression.	*Clin Endocrinol*		(accepted)	

Miyado M, Nakamura M, Miyado K, Ogata T*,et al.	*Mamld1* deficiency significantly reduces mRNA expression levels of multiple genes expressed in mouse fetal Leydig cells but permits normal genital and reproductive development.	*Endocrinology*		(accepted)	
Sekii K*, Itoh H, Ogata T, Iwashima S*	Possible contribution of fetal size and gestational age to myocardial tissue Doppler velocities in preterm fetuses.	*Eur J Obstet Gynecol Reprod Biol*		(accepted)	
Nagasaki K*, Tsuchuya S, Saitoh A, Ogata T, Fukami M.	Neuromuscular symptoms in a patient with familial pseudohypoparathyroidism type Ib diagnosed by methylation-specific multiplex ligation-dependent probe amplification.	*Endocr J*		(accepted)	
Ohishi A*, Ueno D, Matsuoka, H, Kawamoto, F Ogata T	Glucose-6-phosphate dehydrogenase deficiency and adrenal hemorrhage in a Filipino neonate with hyperbilirubinemia.	*Am J Perinatol Reports*		(in press)	
Fuke T, Mizuno S, Nagai T, Hasegawa T, Ogata T*et al.	Molecular and clinical studies in 138 Japanese patients with Silver-Russell syndrome.	*PLoS ONE*		(accepted)	
Ayabe T, Matsubara K, Ogata T, Ayabe A, Murakami N, Nagai T, Fukami M*	Birth seasonality in Prader-Willi syndrome resulting from chromosome 15 microdeletion.	*Am J Med Genet A*		(accepted)	
Fukami M*, Shozu M, Ogata T	Molecular bases and phenotypic determinants of aromatase excess syndrome.	*Int J Endocrinol*	2012	584807	2012
Ogata T*, Sano S, Nagata E, kato F, Fumaki M	*MAMLD1* and 46,XY disorders of sex development.	*Semi Reprod Med*	30 (5)	410–416	2012
Fukami M, Homma K, Hasegawa T, Ogata T*	Backdoor pathway for dihydrotestosterone biosynthesis: implications for normal and abnormal human sex development.	*Dev Dyn*	2012 Oct 16. doi	10.1002/dvdy..23892	[Epub ahead of print]

（作成上の留意事項）

1．「研究成果の刊行に関する一覧表」に記入した書籍又は雑誌は、その刊行物又は別刷り一部を添付すること。

2．研究報告書（当該報告書に含まれる文献等を含む。以下本留意事項において同じ。）は、国立国会図書館及び厚生労働省図書館並びに国立保健医療科学院ホームページにおいて公表されるものであること。研究者等は当該報告書を提出した時点で、公表について承諾したものとすること。

3．日本工業規格A列４番の用紙を用いること。各項目の記入量に応じて、適宜、欄を引き伸ばして差し支えない。

:

NOTE

Advance Publication
doi: 10.1507/endocrj.EJ12-0257

Neuromuscular symptoms in a patient with familial pseudohypoparathyroidism type Ib diagnosed by methylation-specific multiplex ligation-dependent probe amplification

Keisuke Nagasaki[1), 2)]*, Shuichi Tsuchiya[3)]*, Akihiko Saitoh[2)], Tsutomu Ogata[1), 4)] and Maki Fukami[1)]

[1)] *Department of Molecular Endocrinology, National Research Institute for Child Health and Development, Tokyo 157-8535, Japan*
[2)] *Division of Pediatrics, Department of Homeostatic Regulation and Development, Niigata University Graduate School of Medical and Dental Sciences, Niigata 951-8510, Japan*
[3)] *Department of Pediatrics, Ojiya general Hospital, Niigata 947-8641, Japan*
[4)] *Department of Pediatrics, Hamamatsu University School of Medicine, Hamamatsu 431-3192, Japan*

Abstract. Pseudohypoparathyroidism type Ib (PHP-Ib) is a rare genetic disorder characterized by hypocalcemia and hyperphosphatemia due to imprinting defects in the maternally derived *GNAS* allele. Patients with PHP-Ib are usually identified by tetany, convulsions, and/or muscle cramps, whereas a substantial fraction of patients remain asymptomatic and are identified by familial studies. Although previous studies on patients with primary hypoparathyroidism have indicated that hypocalcemia can be associated with various neuromuscular abnormalities, such clinical features have been rarely described in patients with PHP-Ib. Here, we report a 12-year-old male patient with familial PHP-Ib and unique neuromuscular symptoms. The patient presented with general fatigue, steppage gait, and myalgia. Physical examinations revealed muscular weakness and atrophies in the lower legs, a shortening of the bilateral Achilles' tendons and absence of deep tendon reflexes. Laboratory tests showed hypocalcemia, hyperphosphatemia, elevated serum intact PTH level, and impaired responses of urinary phosphate and cyclic AMP in an Ellsworth-Howard test, in addition to an elevated serum creatine kinase level. Clinical features of the patient were significantly improved after 1 month of treatment with alfacalcidol and calcium. Methylation-specific multiplex ligation-dependent probe amplification (MS-MLPA) and subsequent PCR analyses identified a methylation defect at exon A/B of *GNAS* and a microdeletion involving exons 4-6 of the *GNAS* neighboring gene *STX16* in the patient and in his asymptomatic brother. The results suggest that various neuromuscular features probably associated with hypocalcemia can be the first symptoms of PHP-Ib, and that MS-MLPA serves as a powerful tool for screening of GNAS abnormalities in patients with atypical manifestations.

Key words: PHP-Ib, Neuromuscular symptoms, Hypocalcemia, *STX16*, MS-MLPA

PSEUDOHYPOPARATHYROIDISM (PHP; MIM 103580) is a genetically heterogeneous condition characterized by hypocalcemia and hyperphosphatemia resulting from end-organ resistance to PTH [1]. PHP is classified into 2 subtypes, PHP-Ia and -Ib, according to the molecular causes and clinical features of the patients [1]. PHP-Ia results from loss-of-function mutations in the maternally derived *GNAS* gene that encodes the stimulatory G protein α-subunit [1]. Patients with PHP-Ia manifest multiple hormone resistance and characteristic physical stigmata such as short stature, obesity, round face, brachydactyly, subcutaneous ossification, and mild to moderate mental retardation, which are collectively referred to as Albright's hereditary osteodystrophy (AHO) [1, 2].

PHP-Ib is caused by imprinting defects of the maternally derived *GNAS* allele; patients with this condi-

Submitted Jul. 17, 2012; Accepted Oct. 14, 2012 as EJ12-0257
Released online in J-STAGE as advance publication Oct. 25, 2012
Correspondence to: Keisuke Nagasaki, Division of Pediatrics, Department of Homeostatic Regulation and Development, Niigata University Graduate School of Medical and Dental Sciences, Niigata, 951-8510, Japan. E-mail: nagasaki@med.niigata-u.ac.jp
Maki Fukami, Department of Molecular Endocrinology, National Research Institute for Child Health and Development, Tokyo 157-8535, Japan. E-mail: mfukami@nch.go.jp
* K.N. and S.T. contributed equally to this work.

tion show hypomethylation at one or more of the 4 differentially methylated regions (DMRs) of *GNAS* [3-7]. Genetic causes of PHP-Ib include cryptic deletions within the genes neighboring *GNAS*, *STX16* and *NESP55*, and epimutation of *GNAS* DMRs [4, 5]. Patients with PHP-Ib manifest PTH resistance without AHO [1]. These patients are usually identified by hypocalcemia-associated neuromuscular irritability, such as tetany, generalized convulsions, and/or muscle cramps, although a substantial fraction of the patients remain asymptomatic and are identified only by familial studies [6, 7].

Previous studies of patients with primary hypoparathyroidism have shown that hypocalcemia can be associated with various types of neuromuscular symptoms [8, 9]. However, such clinical features have been rarely described in patients with PHP-Ib [10]. Here, we report a Japanese patient with familial PHP-Ib due to an intragenic deletion of *STX16*, who presented with unique neuromuscular symptoms.

Methods

Case report

This male patient was born as the third child to non-consanguineous Japanese parents at 39 weeks of gestation, after an uncomplicated pregnancy and delivery. His birth weight was 3482 g (+1.1 SD) and length 50 cm (+0.7 SD). Neonatal screening tests were normal. His postnatal growth and development were uneventful.

From the age of 6 years, he had general fatigue. At 12 years of age, he was seen by a local doctor because of general fatigue, gait disturbance, and myalgia in the lower legs. He was suspected to have congenital myopathy, and was referred to our clinic for further investigation. His height and weight at the time of examination were 161.4 cm (+1.1 SD) and 42.4 kg (-0.2 SD), respectively. Physical examinations revealed muscular atrophies with weakness in the lower legs, a shortening of the bilateral Achilles' tendons and absence of deep tendon reflexes. He showed a high stepping gait with markedly reduced strength of dorsiflexors of the ankles. Sense of touch and temperature was normal. The Chvostek's sign was positive, while the Trousseau's sign was negative. He had neither AHO stigmata nor episodes of tetany or convulsions. Laboratory examinations revealed hypocalcemia, hyperphosphatemia, and an elevated serum intact PTH level, together with decreased urinary calcium excretions (Table 1). Serum creatine kinase (CK) level was markedly elevated. An Ellsworth-Howard test showed impaired responses of both urinary phosphaturic and cyclic AMP levels (Table 1). The TSH level was slightly elevated, while free T4 and gonadotropin levels were within the normal range. The serum 1,25-dihydroxy vitamin D (1,25(OH)2D) level was mildly elevated. Head computerized tomography (CT) delineated symmetric calcifications of the basal ganglia and thalami, and subcortical calcification of the right middle frontal gyrus. Dual-energy X-ray absorptiometry (DEXA) revealed decreased bone mineral density at the lumbar spine (L2-L4) (0.640 g/cm^2, -2.9 SD). Based on these data, we diagnosed him as having PHP-Ib with neuromuscular symptoms. After 1 month of treatment with alfacalcidol (1.5 μg/day) and calcium lactate (3.0 g/day), his general fatigue, gait disturbance, and myalgia were markedly improved.

The 15-year-old brother of the patient manifested no clinically discernible phenotype; the brother had no gait disturbance or muscle weakness. Furthermore, physical examinations revealed neither muscular atrophy nor neurologic abnormalities. However, laboratory examinations detected an elevated serum intact PTH level, although serum calcium level was within the normal range (Table 1). Thus, the brother was also suspected as having PHP-Ib. The brother manifested mildly elevated serum 1,25(OH)2D level.

The 50-year-old father and 17-year-old sister were clinically normal. The mother, deceased at 49 years of age of an unknown cause, allegedly had no clinical symptoms indicative of PHP. Endocrine studies revealed no abnormalities in the father, sister, or mother (Table 1).

Molecular analyses

This study was approved by the Institutional Review Board Committee at the National Center for Child Health. After obtaining written informed consent, we extracted genomic DNA from leukocytes of the patient and his brother and father.

We examined mutations in the coding region of *GNAS* by direct sequencing, and copy number alternations and methylation defects in the *GNAS*-flanking region by methylation-specific multiplex ligation-dependent probe amplification (MS-MLPA), using a commercially available probe mix (SALSA MLPA kit, ME031-A1) (MRC-Holland, Amsterdam, The Netherlands). To confirm the results of MS-MLPA, we performed PCR analyses using forward and reverse

Table 1 Laboratory findings of the patient and his family members

	Patient	Brother	Father	Mother	Sister	Reference range
Age at the examinations (years)	12	15	50	43	17	
Height (cm) (SDS)	161.4 (+1.1)	171 (+0.1)	N.A.	N.A.	N.A.	
Weight (kg) (SDS)	42.4 (-0.2)	53 (-0.9)	N.A.	N.A.	N.A.	
<Blood>						
Intact PTH (pg/mL)	**430**	**254**	26	44	26	10-65
Calcium (mg/dL)	**6.4**	8.9	9.3	8.7	9.2	8.5-10.2
Phosphate (mg/dL)	**9.1**	**5.2**	2.9	3.8	3.4	2.4-4.3
Magnesium (mg/dL)	1.8	2.0	N.A.	N.A.	N.A.	1.8-2.5
Na (mEq/l)	142	140	N.A.	N.A.	N.A.	135-147
K (mEq/l)	4.1	4.0	N.A.	N.A.	N.A.	3.6-5.0
Creatinine (mg/dL)	0.6	0.7	N.A.	N.A.	N.A.	0.4-1.1
Alb (g/dL)	4.9	4.5	N.A.	N.A.	N.A.	3.9-5.1
CK (IU/L)	**741**	136	N.A.	N.A.	N.A.	0-170
ALP (IU/L)	**1809** (388-1190)[a]	648 (225-680)[a]	N.A.	N.A.	N.A.	
1,25(OH)2D (pg/mL)	**69**	**79**	N.A.	N.A.	N.A.	20-60
TSH (mU/L)	**5.6**	4.1	N.A.	N.A.	N.A.	0.5-5.0
Free T4 (ng/dL)	1.0	1.0	N.A.	N.A.	N.A.	0.9-1.6
<Urine>						
Calcium/Creatinine ratio	**0.004**	**0.008**	N.A.	N.A.	N.A.	0.08-0.20
%TRP	**99.6**	**99.6**	N.A.	N.A.	N.A.	89.6-93.6
<Ellsworth-Howard test>						
Urinary phosphate (mg/2 hrs)[b]	**8.33**	N.A.	N.A.	N.A.	N.A.	≥30
Urinary cAMP (μmol/hr)[c]	**0.029**	N.A.	N.A.	N.A.	N.A.	≥1.0

The conversion factors to the international system of units (SI unit) are as follows: intact PTH 1.0 (ng/liter), serum calcium 0.25 (mmol/liter), serum phosphate 0.3229 (mmol/liter) serum magensium 0.411 (mmol/liter), serum sodium 1.0 (mmol/liter), serum potassium 1.0 (mmol/liter), serum creatine 88.4 (μmol/liter), serum albumin 10 (g/liter), serum 1,25(OH)2D 2.6 (pmol/liter), serum Free T4 12.9 (pmol/liter). Hormone values have been evaluated by the age- and sex-matched Japanese reference data; abnormal data are in bold.

[a] The values in parentheses indicate the age-and sex-matched reference laboratory data.

[b] Urinary phosphate denotes the increment of 2 hours urinary excretion of phosphate after injection of human PTH (100 unit).

[c] Urinary cAMP denote the increment of 1 hour urinary cAMP excretion after injection of human PTH (100 unit).

N.A., not analysed; CK, creatine kinase; 1,25(OH)2D, 1,25-dihydroxy vitamin D; %TRP, % tubular reabsorption of phosphate

primers that hybridize to introns 3 and 6 of *STX16*, respectively [4].

Results

Direct sequence analysis for the patient identified no mutation in the coding region of *GNAS*. However, MS-MLPA revealed decreased peak heights of probes that correspond to exons 5 and 6 of *STX16*, indicating a heterozygous deletion within *STX16*. In addition, MS-MLPA indicated hypomethylation at *GNAS* exon A/B and a normal methylation pattern of the other 3 *GNAS* DMRs (Fig. 1A, B). Subsequent PCR analyses showed the presence of a heterozygous 3 kb deletion involving exons 4-6 of *STX16* (STX16Δexons 4-6) (Fig. 1C). The microdeletion and methylation defect were also observed in the brother, but not in the father. DNA samples of the mother and the sister were not available for genetic analyses.

Discussion

We report here a Japanese patient with PHP-Ib, who was identified by general fatigue, gait disturbance, and myalgia in the lower legs. He showed muscular atrophies in the lower legs, a shortening of the bilateral Achilles' tendons, absence of deep tendon reflexes, and an elevated serum CK value. Such clinical features are indicative of neuromuscular symptoms, although a detailed neurological workup was not performed for

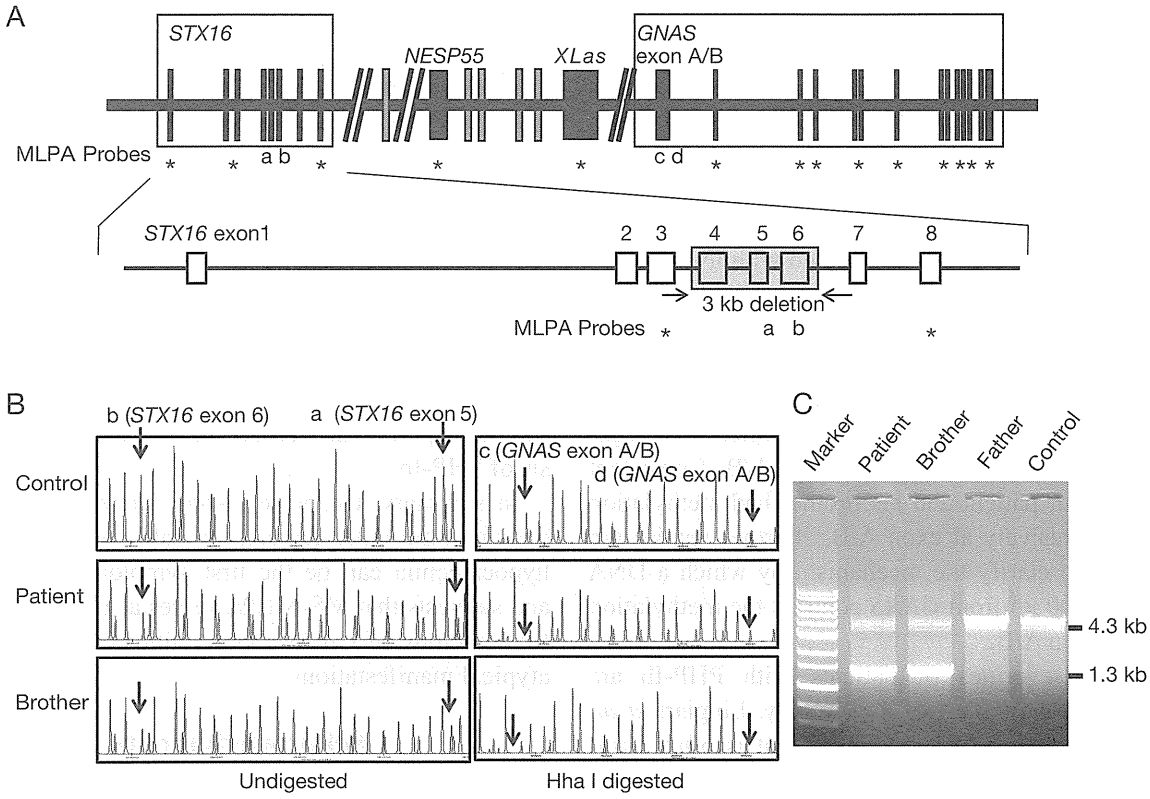

Fig. 1 Molecular analysis of the patient and his family members.

A, Schematic representation of the genomic region around *GNAS*. Upper panel: The loci examined by methylation-specific multiplex ligation-dependent probe amplification (MS-MLPA) are indicated by letters (a-d) and asterisks. Lower panel: Microdeletion identified in the patient and his brother. Horizontal arrows indicate the binding sites of the primers used for PCR analysis.

B. Representative results of MS-MLPA. Left panel: Decreased peak heights with probes a and b in the patient and his brother indicate heterozygous deletion involving exons 5 and 6 of *STX16*. Right panel: Absence of peaks with probes c and d indicate hypomethylation of *GNAS* exon A/B.

C, PCR analysis using a primer pair flanking the deletion. Both the 4.3 kb (wild-type) and 1.3 kb (STX16Δexons4-6) products were amplified from the patient and his brother, while only the 4.3 kb product was obtained from the father and the control individual.

this patient. In this regard, it is noteworthy that peripheral neuropathy and metabolic myopathy have been reported in patients with primary hypoparathyroidism [8, 9], whereas such symptoms have not been described in patients with PHP, except for mildly elevated blood CK and lactate dehydrogenase (LDH) levels in a single case of PHP-Ia [10]. Moreover, *in vitro* experiments showed that calcium concentration affects excitability at neuromuscular junctions [11]. Thus, the neuromuscular symptoms of our patient are likely to be associated with hypocalcemia. A significant improvement in the clinical features of the patient after 1 month of treatment with alfacalcidol and calcium supports this hypothesis. However, we cannot exclude the possibility that other factors such as vitamin D deficiency may also have played a role in the development of these features. Indeed, slightly elevated serum levels of ALP and 1,25(OH)2D in the patient are consistent with mild vitamin D deficiency [12]. On the other hand, since serum 1,25(OH)2D levels were similarly elevated in the patient and his asymptomatic brother, phenotypic variation in this family can not be explained by vitamin D deficiency. These results indicate that neuromuscular features probably associated with hypocalcemia can be the first symptoms of PHP-Ib. Nevertheless, this notion is based on observations of a single case, and

requires further investigations.

Both the patient and his brother carried a heterozygous STX16Δexons4-6. Although DNA samples of the mother were not available for genetic analyses, the absence of the deletion in the father indicated the maternal inheritance of the deletion. It has been shown that maternally inherited STX16Δexons4-6 (STX16Δexons4-6mat) is associated with hypomethylation at *GNAS* exon A/B, whereas *GNAS* epimutations are usually accompanied by methylation defects not only at exon A/B but also at other *GNAS* DMRs [3, 7]. These results suggest that the 3 kb region around exon 4-6 of *STX16* contains a cis-acting element that regulates methylation status at *GNAS* exon A/B. Consistent with this, our patient and his brother had methylation defects exclusively at exon A/B. Further studies are necessary to clarify the mechanism by which a DNA element >200 kb from *GNAS* controls the methylation status at exon A/B.

Clinical severities of patients with PHP-Ib are known to be variable [6, 7]. Notably, Linglart *et al.* have shown that STX16Δexons4-6mat is often associated with a mild phenotype. They found that about 40% of patients carrying this microdeletion remained asymptomatic, and more than 50% of asymptomatic individuals had normocalcemia at the time of diagnosis [7]. Consistent with this, our patient and his brother lacked typical PHP-Ib features such as tetany, generalized convulsions, or muscle cramps. Furthermore, the brother had normocalcemia. These results suggest that physical examinations and measurement of serum calcium levels are not sufficient to identify patients with PHP-Ib, and that genetic analyses or detailed endocrine evaluations, such as measurement of intact PTH levels and an Ellsworth-Howard test, are necessary for patients with atypical manifestations. In this context, although STX16Δexons4-6mat is the most frequent genetic cause of familial PHP-Ib [7], microdeletions affecting *NESP55* as well as epimutations of *GNAS* DMR also account for etiology of PHP-Ib [5, 7]. Since MS-MLPA is capable of detecting both copy number abnormalities and methylation defects in the *GNAS*-flanking region in a single assay, this method should be particularly useful for the molecular diagnosis of PHP-Ib.

In summary, the present study provides that various neuromuscular features probably associated with hypocalcemia can be the first symptoms of PHP-Ib, and suggests that MS-MLPA serves as a powerful tool for screening of *GNAS* abnormalities in patients with atypical manifestations.

Acknowledgments

We thank Dr. K. Kanno (Ojiya General Hospital) for providing us the blood samples of the family. We are also grateful to Ms. T. Tanji and E. Suzuki (National Research Institute for Child Health and Development) for their technical assistance, and Dr. J. Tohyama (Department of Pediatrics, Epilepsy Center, Nishi-Niigata Chuo National Hospital) for his fruitful discussion.

References

1. Levine MA (2000) Clinical spectrum and pathogenesis of pseudohypoparathyroidism. *Rev Endocr Metab Disord* 1: 265-274.
2. Weinstein LS, Yu S, Warner DR, Liu J (2001) Endocrine manifestations of stimulatory G protein alpha-subunit mutations and the role of genomic imprinting. *Endocr Rev* 22: 675-705.
3. Liu J, Litman D, Rosenberg MJ, Yu S, Biesecker LG, et al. (2000) A GNAS1 imprinting defect in pseudohypoparathyroidism type IB. *J Clin Invest* 106: 1167-1174.
4. Bastepe M, Frohlich LF, Hendy GN, Indridason OS, Josse RG, et al. (2003) Autosomal dominant pseudohypoparathyroidism type Ib is associated with a heterozygous microdeletion that likely disrupts a putative imprinting control element of GNAS. *J Clin Invest* 112: 1255-1263.
5. Bastepe M, Frohlich LF, Linglart A, Abu-Zahra HS, Tojo K, et al. (2005) Deletion of the NESP55 differentially methylated region causes loss of maternal GNAS imprints and pseudohypoparathyroidism type Ib. *Nat Genet* 37: 25-27.
6. Kinoshita K, Minagawa M, Takatani T, Takatani R, Ohashi M, et al. (2011) Establishment of diagnosis by bisulfite-treated methylation-specific PCR method and analysis of clinical characteristics of pseudohypoparathyroidism type 1b. *Endocr J* 58: 879-887.
7. Linglart A, Gensure RC, Olney RC, Juppner H, Bastepe M (2005) A novel STX16 deletion in autosomal dominant pseudohypoparathyroidism type Ib redefines the

boundaries of a cis-acting imprinting control element of GNAS. *Am J Hum Genet* 76: 804-814.
8. Kruse K, Scheunemann W, Baier W, Schaub J (1982) Hypocalcemic myopathy in idiopathic hypoparathyroidism. *Eur J Pediatr* 138: 280-282.
9. Goswami R, Bhatia M, Goyal R, Kochupillai N (2002) Reversible peripheral neuropathy in idiopathic hypoparathyroidism. *Acta Neurol Scand* 105: 128-131.
10. Piechowiak H, Grobner W, Kremer H, Pongratz D, Schaub J (1981) Pseudohypoparathyroidism and hypocalcemic "myopathy". A case report. *Klin Wochenschr* 59: 1195-1199.
11. Elmqvist D, Feldman DS (1965) Calcium dependence of spontaneous acetylcholine release at mammalian motor nerve terminals. *J Physiol* 181: 487-497.
12. Bringhurst FR, Demay MB, Kronenberg HM (2011) Hormones and disorders of mineral metabolism. In: Melmed S, Polonsky KS, Larson PR, Kronenberg HM (ed). Williams Textbook of endocrinology (12th). Saunders, Philadelphia: 1237-1304.

Epigenetics 7:10, 1142–1150; October 2012; © 2012 Landes Bioscience

Paternal uniparental disomy 14 and related disorders

Placental gene expression analyses and histological examinations

Masayo Kagami,[1] Kentaro Matsuoka,[2] Toshiro Nagai,[3] Michiko Yamanaka,[4] Kenji Kurosawa,[5] Nobuhiro Suzumori,[6] Yoichi Sekita,[7] Mami Miyado,[1] Keiko Matsubara,[1] Tomoko Fuke,[1] Fumiko Kato,[1,8] Maki Fukami[1] and Tsutomu Ogata[1,8,*]

[1]Department of Molecular Endocrinology; National Research Institute for Child Health and Development; Tokyo, Japan; [2]Departments of Pathology; National Center for Child Health and Development; Tokyo, Japan; [3]Department of Pediatrics; Dokkyo University School of Medicine; Koshigaya, Japan; [4]Department of Integrated Women's Health; St. Luke's International Hospital; Tokyo, Japan; [5]Division of Medical Genetics; Kanagawa Children's Medical Center; Yokohama, Japan; [6]Department of Obstetrics and Gynecology; Nagoya City University Graduate School of Medicine; Nagoya, Japan; [7]Department of Pathology; Graduate School of Medicine; Osaka University, Osaka, Japan; [8]Department of Pediatrics; Hamamatsu University School of Medicine; Hamamatsu, Japan

Keywords: Upd(14)pat, microdeletion, placenta, expression dosage, histopathology, imprinting

Abbreviations: *PEGs*, paternally expressed genes; *MEGs*, maternally expressed genes; DMRs, differentially methylated regions; IG-DMR, *DLK1-MEG3* intergenic DMR; *RTL1as*, *RTL1* antisense; upd(14)pat, paternal uniparental disomy 14; BWS, Beckwith-Wiedemann syndrome; q-PCR, quantitative real-time PCR; CGH, oligoarray comparative genomic hybridization; LM, light microscopic; EM, electron microscopic; IHC, immunohistochemical

Although recent studies in patients with paternal uniparental disomy 14 [upd(14)pat] and other conditions affecting the chromosome 14q32.2 imprinted region have successfully identified underlying epigenetic factors involved in the development of upd(14)pat phenotype, several matters, including regulatory mechanism(s) for *RTL1* expression, imprinting status of *DIO3* and placental histological characteristics, remain to be elucidated. We therefore performed molecular studies using fresh placental samples from two patients with upd(14)pat. We observed that *RTL1* expression level was about five times higher in the placental samples of the two patients than in control placental samples, whereas *DIO3* expression level was similar between the placental samples of the two patients and the control placental samples. We next performed histological studies using the above fresh placental samples and formalin-fixed and paraffin-embedded placental samples obtained from a patient with a maternally derived microdeletion involving *DLK1*, the-IG-DMR, the *MEG3*-DMR and *MEG3*. Terminal villi were associated with swollen vascular endothelial cells and hypertrophic pericytes, together with narrowed capillary lumens. DLK1, RTL1 and DIO3 proteins were specifically identified in vascular endothelial cells and pericytes, and the degree of protein staining was well correlated with the expression dosage of corresponding genes. These results suggest that *RTL1as*-encoded microRNA functions as a repressor of *RTL1* expression, and argue against *DIO3* being a paternally expressed gene. Furthermore, it is inferred that DLK1, DIO3 and, specially, RTL1 proteins, play a pivotal role in the development of vascular endothelial cells and pericytes.

Introduction

Human chromosome 14q32.2 region carries a cluster of imprinted genes including protein coding paternally expressed genes (*PEGs*) such as *DLK1* and *RTL1* (alias *PEG11*) and non-coding maternally expressed genes (*MEGs*) such as *MEG3* (alias *GTL2*) and *RTL1as* (*RTL1* antisense encoding microRNAs).[1,2] The 14q32.2 imprinted region also harbors two differentially methylated regions (DMRs), i.e., the germline-derived primary *DLK1-MEG3* intergenic DMR (IG-DMR) and the postfertilization-derived secondary *MEG3*-DMR.[1,2] Both DMRs are hypermethylated after paternal transmission and hypomethylated after maternal transmission in the body, whereas in the placenta the IG-DMR alone remains as a DMR and the *MEG3*-DMR is rather hypomethylated.[2] We have previously revealed that the hypomethylated IG-DMR and *MEG3*-DMR of maternal origin function as imprinting control centers in the placenta and the body, respectively, and that the IG-DMR functions hierarchically as an upstream regulator for the methylation pattern of the *MEG3*-DMR on the maternally inherited chromosome in the body, but not in the placenta.[3]

*Correspondence to: Tsutomu Ogata; Email: tomogata@hama-med.ac.jp
Submitted: 06/21/12; Revised: 08/20/12; Accepted: 08/22/12
http://dx.doi.org/10.4161/epi.21937

Consistent with these findings, paternal uniparental disomy 14 [upd(14)pat] results in a unique phenotype characterized by facial abnormality, small bell-shaped thorax with coat hanger appearance of the ribs, abdominal wall defects, placentomegaly and polyhydramnios.[2,4] We have studied multiple patients with upd(14)pat and related conditions, such as epimutations of the maternally derived DMRs and various types of microdeletions involving the maternally inherited imprinted region, suggesting that markedly increased *RTL1* expression is the major underlying factor for the development of upd(14)pat-like phenotype.[2] The notion of excessive *RTL1* expression is primarily based on the following mouse data indicating a trans-acting repressor function of *Rtl1as*-encoded microRNAs for *Rtl1* expression: (1) targeted deletion of the maternally derived IG-DMR causes maternal to paternal epigenotypic switch of the imprinted region, with ~4.5 times rather than ~2 times of *Rtl1* expression as well as ~2 times of *Dlk1* expression and nearly absent *Megs* expression, in the presence of two functional copies of *Pegs* and no functional copy of *Megs*[5] and; (2) targeted deletion of the maternally derived *Rtl1as* results in 2.5–3.0 times of *Rtl1* expression, in the presence of a single functional copy of *Rtl1*.[6] Similarly, in the human, typical upd(14)pat phenotype is observed in patients with epimutations that are likely associated with markedly increased *RTL1* expression because of the combination of two functional copies of *RTL1* and no functional copy of *RTL1as*, whereas relatively mild upd(14)pat-like phenotype is found in patients with maternally inherited microdeletions involving *RTL1as* that are likely accompanied by moderately elevated *RTL1* expression because of the combination of a single functional copy of *RTL1* and no functional copy of *RTL1as*.[2]

Human imprinting disorders are usually associated with placental abnormalities. For example, Beckwith-Wiedemann syndrome (BWS) and upd(14)pat are associated with placentomegaly,[4,7] and Silver-Russell syndrome is accompanied by hypoplastic placenta.[8] Similarly, mouse imprinting aberrations also usually affect placental growth and development.[9] In agreement with this, virtually all the imprinted genes studied to date are expressed in the placenta and play a pivotal role in the placental growth and development,[10] although placental structure is more or less different between placental animals.[11]

However, several matters remain to be clarified in upd(14)pat and related conditions. For example, it is unknown whether human *RTL1* expression is actually elevated in the absence of functional *RTL1as*-encoded microRNAs. It is also unknown whether *DIO3* is a *PEG*, although mouse *Dio3* has been shown to undergo partial imprinting.[12] In this regard, while we examined fresh blood cells, cultured skin fibroblasts and formalin-fixed and paraffin-embedded placental and body samples obtained from patients with upd(14)pat-like phenotype, precise assessment of *RTL1* and *DIO3* expression levels was impossible because of extremely low *RTL1* and *DIO3* expression levels in fresh blood cells and cultured skin fibroblasts and poor quality of RNAs extracted from paraffin-embedded tissues.[2,3] In addition, while cSNP genotyping has demonstrated paternal *DLK1* and *RTL1* expression and maternal *MEG3* expression in the body and the placenta,[2,3] no informative cSNP data showing paternal *DIO3* expression have been obtained.[2,3] Furthermore, although standard light microscopic (LM) examinations have been performed using formalin-fixed and paraffin-embedded placental samples, fine placental histopathological studies, such as electron microscopic (EM) examinations and immunohistochemical (IHC) examinations, remain to be performed.

To examine these unresolved matters, fresh placental tissues are highly useful, because precise quantitative real-time PCR (q-PCR) analyses and EM studies can be performed with fresh placentas. Thus, we performed q-PCR analyses and EM studies, as well as IHC studies with RTL1 antibodies produced by ourselves and commercially available DLK1 and DIO3 antibodies, using fresh placental samples obtained from two previously reported patients with prenatally diagnosed upd(14)pat.[13,14] We also performed IHC studies using formalin-fixed and paraffin-embedded placental samples obtained from a previously reported patient with a microdeletion involving *DLK1*, but not *RTL1* and *DIO3*,[2] to compare the placental protein expression levels between upd(14)pat and the microdeletion. Furthermore, we also studied a hitherto unreported patient with an unbalanced translocation involving the 14q32.2 imprinted region, to obtain additional data regarding the *RTL1-RTL1as* interaction and the primary factor for the development of upd(14)pat phenotype.

Results

Patients and samples. This study consisted of three previously reported patients with typical body and placental upd(14)pat phenotype and a normal karyotype (cases 1–3),[2,13-15] and a new patient with various non-specific features and a 46,XX,der(17)t(14;17)(q31;p13) karyotype accompanied by three copies of the distal 14q region and a single copy of the terminal 17p region (case 4) . Clinical phenotypes of cases 1–4 are summarized in **Table S1**. In brief, cases 1 and 2 were suspected to have upd(14)pat phenotype including bell-shaped thorax by prenatal ultrasound studies performed for polyhydroamnios, and were confirmed to have upd(14)pat by microsatellite analysis after birth. Case 3 was found to have typical upd(14)pat phenotype during infancy and was shown to have a maternally derived microdeletion affecting the chromosome 14q32.2 imprinted region. Case 4 had growth failure, developmental delay, multiple non-specific anomalies, and omphalocele. There was no history of polyhydramnios or placentomegaly. Thus, except for omphalocele, case 4 had no upd(14)pat-like phenotype. The parental karyotype was normal, indicating a de novo occurrence of the unbalanced translocation.

We obtained fresh placental samples immediately after birth from prenatally diagnosed cases 1 and 2 for molecular studies using genomic DNA and RNA, and fresh leukocyte samples from cases 1, 2 and 4 and their parents for molecular studies using genomic DNA. The fresh placental samples of cases 1 and 2 were also utilized for histopathological examinations, together with formalin-fixed and paraffin-embedded placental samples of case 3. For controls, we obtained three fresh placentas at 37 weeks of gestation, and fresh leukocytes from three adult subjects; for molecular studies using placentas, we prepared pooled samples

consisting of an equal amount of DNA or RNA extracted from each placenta.

Molecular studies in cases 1 and 2. We performed microsatellite analysis for 19 loci on chromosome 14 and bisulfite sequencing for the IG-DMR (CG4 and CG6) and the *MEG3*-DMR (CG7), using placental and leukocyte genomic DNA samples; while microsatellite analysis had been performed for 15 loci in case 1 and 16 loci in case 2, only leukocyte genomic DNA samples were examined in the previous study.[15] Consequently, we identified two peaks for *D14S609* and single peaks for the remaining loci in case 1 (the combination of paternal heterodisomy and isodisomy), and single peaks for all the examined loci in case 2 (apparently full paternal isodisomy) (**Table S2**). Furthermore, no trace of maternally inherited peak was identified in both placental and leukocyte genomic DNA samples (**Fig. 1**). Bisulfite sequencing showed that both the IG-DMR and the *MEG3*-DMR were markedly hypermethylated in the leukocytes of cases 1 and 2, whereas in the placental samples the IG-DMR was obviously hypermethylated and the *MEG3*-DMR was grossly hypomethylated to an extent similar to that identified in control placentas (**Fig. 2**). Furthermore, q-PCR analysis for placental RNA samples revealed that *DLK1*, *RTL1*, and *DIO3* expression levels were 3.3 times, 6.1 times and 1.9 times higher in the placental samples of case 1 than in the control placental samples, respectively, and were 3.1 times, 9.4 times and 1.7 times higher in the placental samples of case 2 than in the control placental samples, respectively (**Fig. 3A**). By contrast, the expressions of all *MEGs* examined were virtually absent in the placental samples of cases 1 and 2. PCR products were sufficiently obtained after 30 cycles for the fresh placental as well as leukocyte samples, consistent with high quality of DNA and RNA obtained from fresh materials.

Molecular studies in case 3. Detailed molecular findings have already been reported previously.[2] In brief, microsatellite analysis revealed biparentally derived homologs of chromosome 14, and a deletion analysis demonstrated a maternally inherited 108,768 bp microdeletion involving *DLK1*, the IG-DMR, the *MEG3*-DMR, and *MEG3*, but not affecting *RTL1*/*RTL1as*. Since loss of the DMRs causes maternal to paternal epigenotypic alteration,[2] it is predicted that case 3 has a single functional copy of *DLK1* and two functional copies of *RTL1* and *DIO3*, as well as no functional copy of *RTL1as* and other *MEGs*. Bisulfite sequencing showed that both the IG-DMR and the *MEG3*-DMR were markedly hypermethylated in leukocytes, whereas in the formalin-fixed and paraffin-embedded placental samples the IG-DMR was obviously hypermethylated and the *MEG3*-DMR was comprised of roughly two-thirds of hypermethylated clones and roughly one-third of hypomethylated clones. In addition, RT-PCR analysis for such placental samples indicated positive *PEGs* (especially *RTL1*) expression and absent *MEGs* expression. For the formalin-fixed and paraffin-embedded placental samples, PCR products could be obtained only after 35 cycles, because of poor quality (severe degradation) of DNA and RNA.

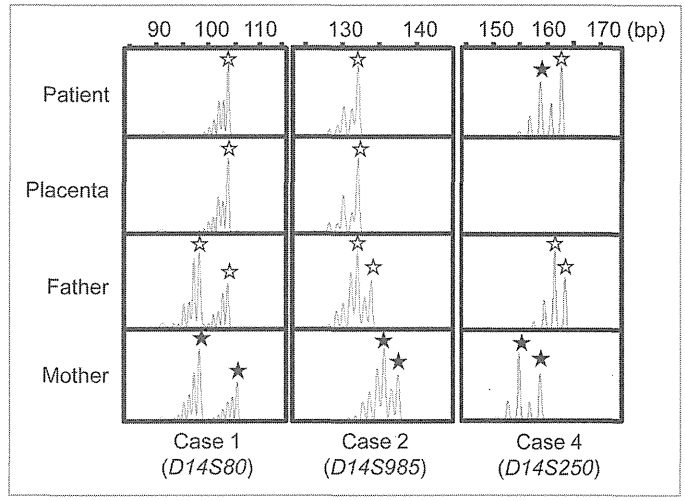

Figure 1. Representative results of microsatellite analysis, using leukocyte genomic DNA samples of the patient and the parents and placental genomic DNA samples. In cases 1 and 2, one of the two paternal peaks is inherited by the patients and the placentas, and no trace of maternal peaks is identified. In case 4, both paternally and maternally derived peaks are found in the patient, with the paternally derived long peak being larger than the maternally inherited short peak.

Molecular findings in case 4. We examined the presence or absence of the 14q32.2 imprinted region on the der(17) chromosome (**Fig. 4**). Oligoarray comparative genomic hybridization (CGH) indicated three copies of a ~19.6 Mb 14q31–qter region, and FISH analysis for four segments around the chromosome 14q32.2 imprinted region delineated positive signals on the der(17) chromosome as well as on the normal chromosome 14 homologs. This demonstrated the presence of the 14q32.2 imprinted region on the der(17) chromosome. In addition, similar oligoarray CGH and FISH analysis revealed loss of a ~455 kb region from the distal chromosome 17p (**Fig. S1**).

Thus, we investigated the parental origin of the translocated 14q distal region. Microsatellite analysis for *D14S250* and *D14S1007* on the translocated 14q distal region delineated biparentally derived two peaks, with paternally derived long PCR products showing larger peaks than maternally derived short PCR products (**Fig. 1**; **Table S2**). Since short products are usually more easily amplified than long products, this indicated paternal

Figure 2 (See opposite page). Bisulfite sequencing analysis of the IG-DMR (CG4 and CG6) and the *MEG3*-DMR (CG7), using leukocyte and placental genomic DNA samples. Filled and open circles indicate methylated and unmethylated cytosines at the CpG dinucleotides, respectively. Upper part: structure of CG4, CG6, and CG7. Pat, paternally derived chromosome; Mat, maternally derived chromosome. The PCR products for CG4 (311 bp) harbor 6 CpG dinucleotides and a G/A SNP (*rs12437020*), those for CG6 (428 bp) carry 19 CpG dinucleotides and a C/T SNP (*rs10133627*) and those for CG7 (168 bp) harbor 7 CpG dinucleotides. Lower part: the results of cases 1, 2, 4 and a control subject. Each horizontal line indicates a single subcloned allele. The control data represent the methylation patterns obtained with a leukocyte genomic DNA sample extracted from a single subject heterozygous for the G/A SNP (*rs12437020*) (body) and those obtained with a pooled DNA sample consisting of an equal amount of genomic DNA extracted from three control placentas homozygous for that SNP.

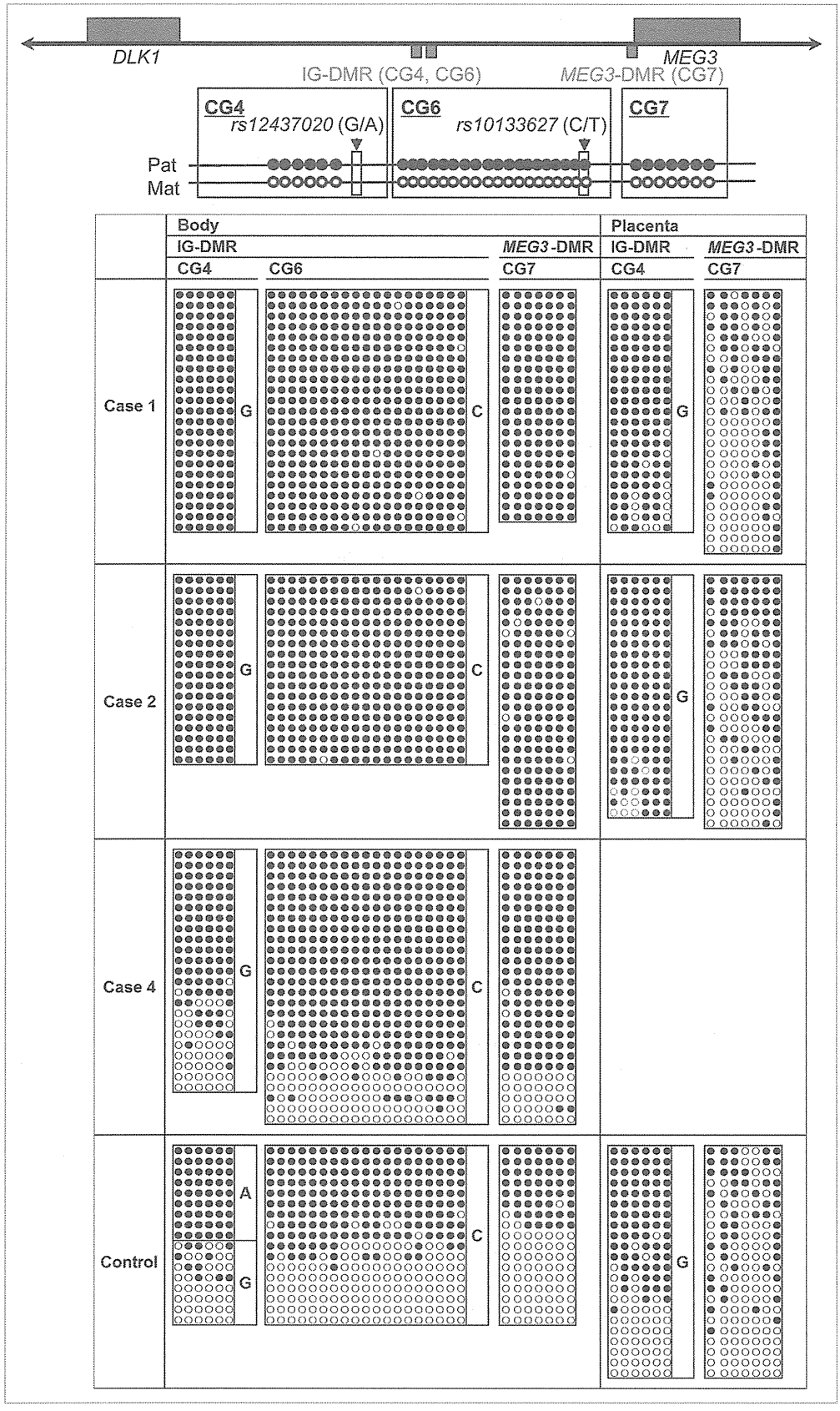

Figure 2. For figure legend, see page 1144.

origin of the der(17) chromosome harboring the chromosome14q32.2 imprinted region. Consistent with this, bisulfite sequencing showed moderate hypermethylation of the IG-DMR and the *MEG3*-DMR (**Fig. 2**).

Placental histopathological studies. We performed LM and EM studies, and IHC examinations (**Fig. 5**). LM examinations showed proliferated chorionic villi in cases 1–3. Capillary lumens were irregularly dilated with thickened endothelium in the stem to intermediate villi, but not in the terminal villi. Immature villi were present in case 3, probably because of 30 weeks of gestational age. Chorangioma was also identified in case 3. There was no villous chorangiosis, edematous change of villous stroma, or mesenchymal dysplasia characterized by grapelike vesicles in cases 1–3. Although the terminal villi exhibited no definitive abnormalities in the LM studies, EM examinations revealed swelling of vascular endothelial cells and hypertrophic change of pericytes in the terminal villi, together with narrowed capillary lumens, in cases 1 and 2.

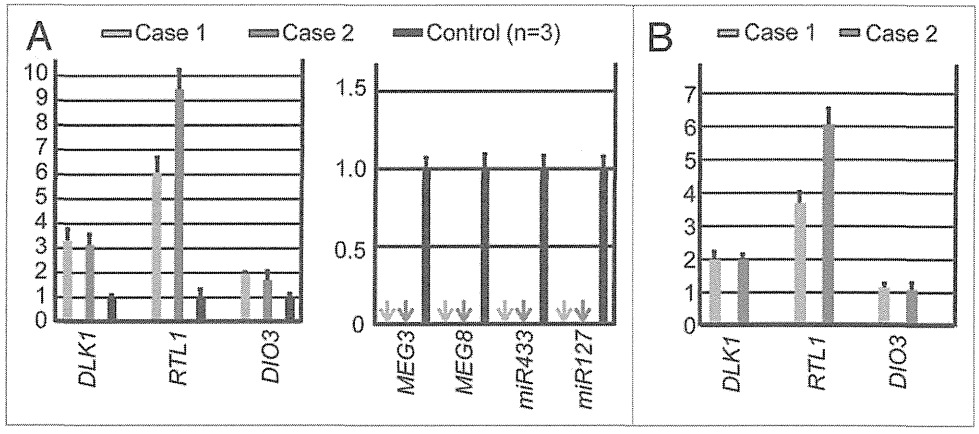

Figure 3. Quantitative real-time PCR analysis using placental samples. For a control, a pooled RNA sample consisting of an equal amount of total RNA extracted from three fresh control placentas was utilized. (**A**) Relative mRNA expression levels for *DLK1*, *RTL1*, and *DIO3* against *GAPDH* (mean ± SE) and lack of *MEGs* expression (indicated by arrows) (*miR433* and *miR127* are encoded by *RTL1as*) in the placental samples of cases 1 and 2. (**B**) Relative mRNA expression levels for *DLK1*, *RTL1*, and *DIO3* against *GAPDH* (mean ± SE), in the equal amount of expression positive placental cells (vascular endothelial cells and pericytes) of cases 1 and 2 (corrected for the difference in the relative proportion of expression positive cells between the placental samples of cases 1 and 2 and the control placental samples, on the assumption that the *DLK1* expression level is "simply doubled" in the expression positive placental cells of case 1 and 2).

IHC examinations identified RTL1, DLK1 and DIO3 protein expressions in the vascular endothelial cells and pericytes of chorionic villi, but not in the cytotrophoblasts, syncytiotrophoblasts, and stromal cells, in the placentas of cases 1–3 and in the control placenta. The PEGs protein expression level was variable in the control placenta, with moderate DLK1 expression, high RTL1 expression, and low DIO3 expression. Furthermore, DLK1 protein expression was apparently stronger in the placentas of cases 1 and 2 than in the placenta of case 3 and the control placenta, RTL1 protein expression was obviously stronger in the placentas of cases 1–3 than in the control placenta, and DIO3 protein expression was apparently similar between the placentas of cases 1–3 and the control placenta.

Discussion

We studied placental samples obtained from cases 1–3 with typical body and placental upd(14)pat phenotype. In this regard, the microsatellite data suggest that upd(14)pat with heterodisomic and isodisomic loci in case 1 was caused by trisomy rescue or gamete complementation, and that upd(14)pat with isodisomic loci alone in case 2 resulted from monosomy rescue or postzygotic mitotic error, although it is possible that heterodisomic locus/loci remained undetected in case 2.[15] Notably, there was no trace of a maternally inherited locus indicative of the presence of trisomic cells or normal cells with biparentally inherited chromosome 14 homologs in the placentas as well as in the leukocytes of cases 1 and 2. In addition, the microdeletion of case 3 has been shown to be inherited from the mother with the same microdeletion.[2] These findings imply that the placental tissues as well as the leukocytes of cases 1–3 almost exclusively, if not totally, consisted of cells with upd(14)pat or those with the microdeletion.

The q-PCR analysis was performed for the fresh placental samples of cases 1 and 2. In this context, two matters should be pointed out. First, the proportion of vascular endothelial cells and pericytes expressing *DLK1*, *RTL1*, and *DIO3* would be somewhat variable among samples, because only a small portion of the placenta was analyzed. This would be relevant to the some degree of difference in the expression levels between the placental samples of cases 1 and 2. Second, the relative proportion of vascular endothelial cells and pericytes expressing *DLK1*, *RTL1*, and *DIO3* would be higher in the placental samples of cases 1 and 2 than in the control placental samples, because the placentas of cases 1 and 2 were accompanied by proliferation of the chorionic villi with such expression positive cells. Thus, it would be inappropriate to perform a simple comparison of relative expression levels against *GAPDH* between the placental samples of cases 1 and 2 and the control placental samples. Indeed, although a complex regulatory mechanism(s), as implicated for the *RTL1* expression,[1,2] is unlikely to be operating for the *DLK1* expression, the relative *DLK1* expression level was 3.3 times and 3.1 times, not 2 times, higher in the placental samples of cases 1 and 2 than in the control placental samples, respectively (**Fig. 3A**). Assuming that *DLK1* expression level is simply doubled in expression positive cells of cases 1 and 2, it is predicted that the relative proportion of such expression positive cells is 1.65 times (3.3 ÷ 2.0) and 1.55 times (3.1 ÷ 2.0) larger in the placental samples of cases 1 and 2 than in the control placental samples, respectively. Thus, the expression level against *GAPDH*

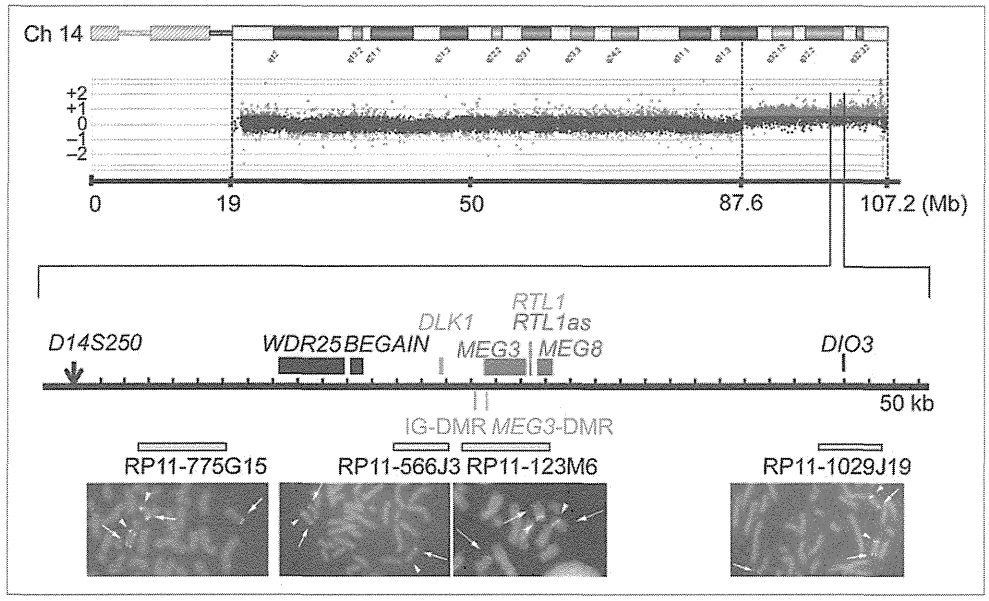

Figure 4. Array CGH and FISH analysis for the distal chromosome 14 region in case 4. In CGH analysis, the black, the red, and the green dots denote signals indicative of the normal, the increased (> +0.5), and the decreased (< −1.0) copy numbers, respectively. In FISH analysis, red signals (arrows) are derived from the probes detecting the various parts of the 14q32.2 imprinted region (the physical positions are indicated with yellow bars), and the green signals (arrowheads) are derived from an RP11–566I2 probe for 14q11.2 used as an internal control.

in the equal amount of expression positive cells is estimated as 3.69 times (6.1 ÷ 1.65) increased for *RTL1* and 1.15 times (1.9 ÷ 1.65) increased for *DIO3* in case 1, and as 6.06 times (9.4 ÷ 1.55) increased for *RTL1* and 1.09 times (1.7 ÷ 1.55) increased for *DIO3* in case 2 (**Fig. 3B**).

Thus, the expression data are summarized as follows (**Fig. 6**). First, it is inferred that the relative *RTL1* expression level is markedly (~5 times) increased in the expression positive cells of the placentas with upd(14)pat, as compared with the control placentas. This degree of elevation is grossly similar to that identified in the body of mice with the targeted deletion of the maternally derived IG-DMR (~4.5 times).[5] Such a markedly increased *RTL1* expression would be explained by assuming that *RTL1as*-encoded microRNAs (e.g., *miR433* and *miR127*) function as a repressor for *RTL1* expression through the RNAi mechanism, as has been indicated for the mouse *Rtl1-Rtl1as* interaction.[16,17] Second, it is unlikely that *DIO3* is solely expressed from the paternally inherited allele, although it remains to be determined whether *DIO3* undergoes partial imprinting like mouse *Dio3*[12] or completely escapes imprinting. In either case, the results would explain why patients with upd(14)pat and upd(14)mat lack clinically recognizable thyroid disorders,[2] although *DIO3* plays a critical role in the inactivation of thyroid hormones.[18]

This study provides further support for a critical role of excessive *RTL1* expression in the development of upd(14)pat phenotype (**Fig. 6**). Indeed, markedly (~5 times) increased *RTL1* expression is shared in common by cases 1–3 with typical upd(14)pat body and placental phenotype. In this context, it is notable that case 4 had no clinically recognizable upd(14)pat body and placental phenotype, except for omphalocele. This would imply that a single copy of *RTL1as* can almost reduce the *RTL1* expression dosage below the threshold level for the development of upd(14)pat phenotype by exerting a trans-acting repressor effect on the two functional copies of *RTL1*. By contrast, the relevance of *DLK1* to upd(14)pat phenotype is unlikely, because case 3 exhibited typical upd(14)pat phenotype in the presence of a single functional copy of *DLK1*, and case 4 showed no upd(14)pat phenotype except for omphalocele in the presence of two functional copies of *DLK1*. Similarly, if *DIO3* were more or less preferentially expressed from paternally inherited allele, the relevance of *DIO3* to upd(14)pat phenotype would also remain minor, if any. Case 4 had no upd(14)pat phenotype except for omphalocele in the presence of with two copies of *DIO3* of paternal origin. It should be pointed out, however, that the absence of *MEGs* expression may have a certain effect on the development of upd(14)pat phenotype.

The placental histological examinations revealed several informative findings. First, DLK1, RTL1, and DIO3 proteins were specifically identified in vascular endothelial cells and pericytes of chorionic villi in the control placenta, with RTL1 protein being most strongly expressed. These results, together with abnormal LM and EM findings of such cells in cases 1–3, suggest that these proteins, especially RTL1 protein, plays a pivotal role in the development of endothelial cells and pericytes. In this regard, it may be possible that the endothelial thickening and resultant narrowing the capillary lumens in the terminal villi have resulted in the dilatation of the stem to intermediate portions of the chorionic villi.

Second, the degree of protein staining was well correlated with the expression dosage of corresponding genes. In this regard, since characteristic macroscopic and microscopic placental features were identified in cases 1–3 who shared markedly elevated RTL1 protein expression, this is consistent with the notion that upd(14)pat phenotype is primarily caused by the markedly

elevated *RTL1* expression.[2] Indeed, DLK1 protein expression was not exaggerated in case 3 with typical upd(14)pat phenotype, and DIO3 protein expression was not enhanced in cases 1–3. It may be possible, however, that the abnormality of placental structures may have resulted in a difference in immunostaining without an actual change in gene expression. This point awaits further investigations.

Third, villous chorangiosis, stromal expansion, and mesenchymal dysplasia were not identified in the placental samples of cases 1–3, although such a lesion(s) may have existed in non-examined portions. Notably, such lesions are frequently observed in placentas of patients with BWS.[19-21] Thus, while both upd(14)pat and BWS are associated with placentomegaly and polyhydroamnios, characteristic histological findings appear to be different between upd(14)pat and BWS.

This study would also provide useful information on the methylation patterns of the *MEG3*-DMR in the placenta. Our previous studies using formalin-fixed and paraffin-embedded placental samples revealed that roughly two-thirds of clones were hypermethylated and the remaining roughly one-third of clones were hypomethylated in case 3 as well as in the previously reported patients with upd(14)pat (not cases 1 and 2) and epimutation (hypermethylation of the IG-DMR and the *MEG3*-DMR of maternal origin), and that roughly one-third of clones were hypermethylated and the remaining roughly two-thirds of clones were hypomethylated in control placental samples (see Fig. S2C in ref. 2). However, this study showed that the *MEG3*-DMR was grossly hypomethylated in the fresh placental samples of cases 1 and 2, with an extent similar to that identified in the fresh control placental samples. In this regard, it is notable that PCR products could be obtained only after 35 cycles for the formalin-fixed and paraffin-embedded placental samples and were sufficiently obtained after 30 cycles for the fresh placental samples. Thus, several specific clones may have been selectively amplified in the previous study. Furthermore, it may be possible that efficacy of bisulfite treatment (conversion of unmethylated cytosine into uracils and subsequently thymines) may be insufficient for the formalin-fixed and paraffin-embedded placental samples. Thus, it appears that the present data denote precise methylation patterns of the *MEG3*-DMR in the placenta.

In summary, the present study provides useful clues for the clarification of regulatory mechanism for the *RTL1* expression, imprinting status of *DIO3* and characteristic placental histological findings in patients with upd(14)pat and related conditions. Further studies will help improve our knowledge about upd(14)pat and related conditions.

Methods

Ethical approval. This study was approved by the Institutional Review Board Committees of each investigator, and performed after obtaining written informed consent.

Primers. Primers utilized in this study are summarized in Table S3.

Sample preparation for molecular studies. Genomic DNA samples were obtained from leukocytes using FlexiGene DNA Kit (Qiagen) and from placental samples using ISOGEN (Nippon Gene). Transcripts of *DLK1, MEG3, RTL1, MEG8* and *DIO3* were isolated with ISOGEN (Nippon Gene), and *microRNAs* were extracted with mirVana™ miRNA Isolation Kit (Ambion). After DNase treatment, cDNA samples for *DLK1, MEG3, MEG8* and *DIO3* were prepared with oligo(dT) primers from 1 μg of RNA using Superscript III Reverse Transcriptase (Invitrogen), and those of *microRNAs* were synthesized from 300 ng of RNA using TaqMan MicroRNA Reverse Transcription Kit (Applied Biosystems). For *RTL1*, 3'-RACE was utilized to prevent amplification of *RTL1as*; cDNA was synthesized from 1 μg of RNA using Superscript III Reverse Transcriptase with a long primer hybridizing to poly A site and introducing the adaptor sequence. Lymphocyte metaphase spreads for FISH analysis were prepared from leukocytes using colcemide (Invitrogen).

Molecular studies. Microsatellite analysis for 19 loci on chromosome 14, methylation analysis for the IG-DMR and

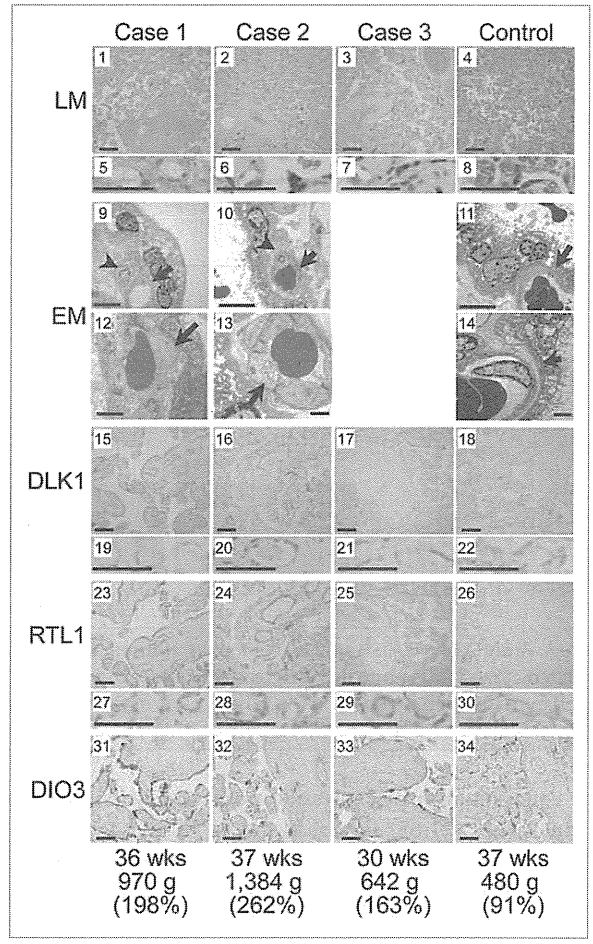

Figure 5. Histological examinations. LM, light microscopic examinations; EM, electron microscopic examinations; DLK1, RTL1 and DIO3, immunohistochemical examinations for the corresponding proteins. The arrows and arrowheads in the EM findings indicate endothelial cells and pericytes, respectively. Scale bars represent 100 μm for 1–4, 15–18, 23–26 and 31–34, 50 μm for 5–8, 19–22 and 27–30, 5 μm for 9–11 and 2 μm for 12–14. Gestational age, placental weight, and % placental weight assessed by the gestational age-matched Japanese references for placental weight[4,22] are described.

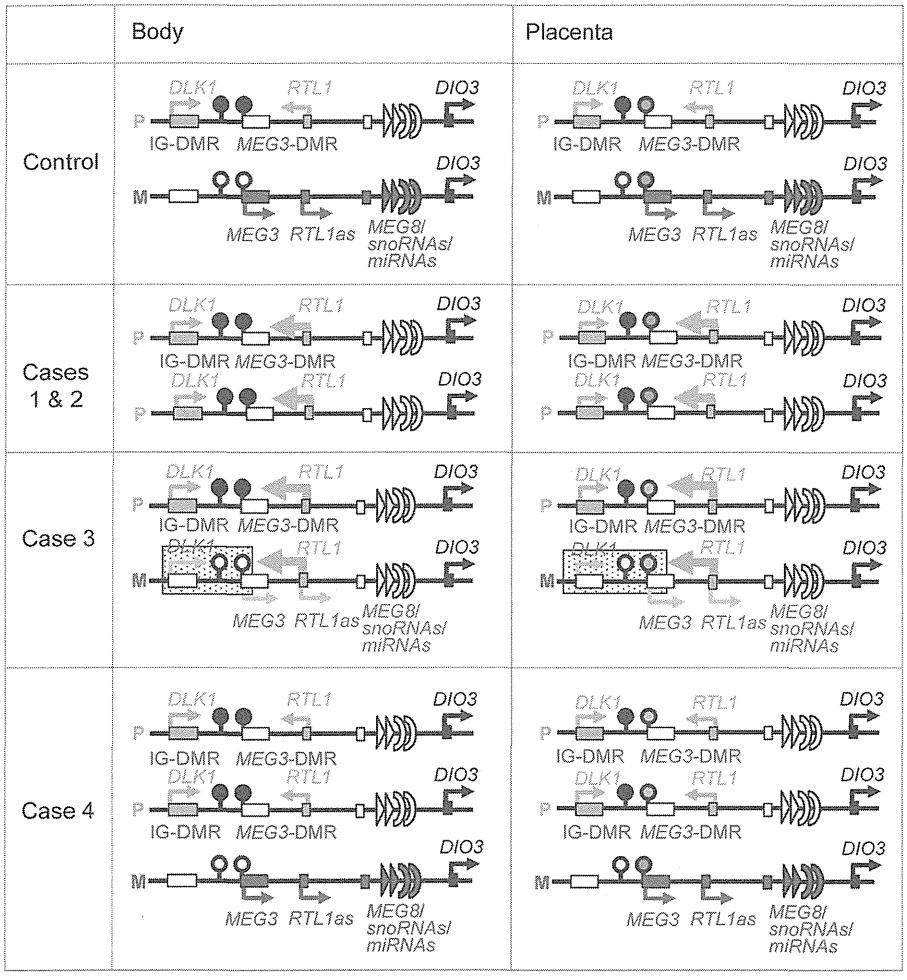

Figure 6. Schematic representation of the chromosome 14q32.2 imprinted region in a control subject, cases 1 and 2 with upd(14)pat, case 3 with a microdeletion (indicated by stippled rectangles), and case 4 with two copies of the imprinted region of paternal origin and a single copy of the imprinted region of maternal origin. This figure has been constructed using the present results and the previous data.[2,3] P, paternally derived chromosome; M, maternally derived chromosome. Filled and open circles represent hypermethylated and hypomethylated DMRs, respectively; since the *MEG3*-DMR is grossly hypomethylated and regarded as non-DMR in the placenta, it is painted in gray. *PEGs* (*DLK1* and *RTL1*) are shown in blue, *MEGs* (*MEG3*, *RTL1as*, *MEG8*, *snoRNAs* and *miRNAs*) in red, a probably non-imprinted gene (*DIO3*) in black, and non-expressed genes in white. Thick arrows for *RTL1* in cases 1–3 represent increased *RTL1* expression that is ascribed to loss of functional microRNA-containing *RTL1as* as a repressor for *RTL1*.

the *MEG3*-DMR, and FISH analyses for the 14q32.2 region were performed as described previously.[2,3] For FISH analysis of 17p13.3, a 17p sub-telomere probe and an RP11–411G7 probe for the 17p13.3 region were utilized, together with a CEP17 probe for the 17p11.1 region utilized as an internal control. The 17p sub-telomere probe was detected according to the manufacture's protocol, the RP11–411G7 probe was labeled with digoxigenin and detected by rhodamine anti-digoxigenin, and the CEP17 control probe was labeled with biotin and detected by avidin conjugated to fluorescein isothiocyanate. Quantitative real-time PCR analysis was performed on an ABI PRISM 7000 (Applied Biosystems) using TaqMan real-time PCR probe primer mixture for the following genes (assay No: Hs00171584 for *DLK1,* Hs00292028 for *MEG3*, Hs00419701 for *MEG8* and Hs00704811 for *DIO3*; assay ID: 001028 for *miR433* and 000452 for *miR127*). For *RTL1*, q-PCR analysis was performed with a forward primer hybridized to the sequence of *RTL1* and a reverse primer hybridized to the adaptor sequence. Fifty nanograms of cDNA in a 50 μl reaction mixture contacting 2× KOD FX buffer (Toyobo), 2.0 mM dNTP mixture (Toyobo), KOD FX (Toyobo), SYBR Green I (Invitrogen), and primer set for *RTL1* were subjected to the ABI PRISM 7000. Data were normalized against *GAPDH* (catalog No: 4326317E) for *DLK1, MEG3*, *MEG8*, *RTL1*, and *DIO3*, and against *RNU48* (assay ID: 0010006) for *microRNAs*. The expression studies were performed three times for each sample. Oligoarray CGH was performed using 1× 1M format Human Genome Array (Catalog No G4447A) (Agilent Technologies).

Histopathogical analysis. Placental samples were fixed with 20% buffered formaldehyde at room temperature and embedded in paraffin wax according to standard protocols for LM examinations. Then, sections of 3 μm thick were stained with hematoxylin-eosin. For EM examinations, fresh placental tissues were fixed with phosphate-buffered 2.5% glutaraldehyde, postfixed in 1% osmium tetroxide, and embedded in Epon 812 (catalog No. R3245, TAAB). Semithin sections were stained with 1% methylene blue, and ultrathin sections were double-stained with uranyl acetate and lead citrate. Subsequently, they were examined with a Ninhon Denshi JEM-1230 electron microscope.

For IHC analysis, sections of 3 μm thick were prepared by the same methods utilized for the LM examinations, and were examined with rabbit anti human DLK1 polyclonal antibody at 1:100 dilutions (catalog No 10636-1-AP, ProteinTech Group), rabbit anti human RTL1 polyclonal antibody at 1:200 dilutions, and rabbit anti human DIO3 polyclonal antibody at 1:50 dilutions (catalog No ab102926, abcam); anti human RTL1 polyclonal antibody was produced by immunizing rabbits with the synthesized RTL1 peptide (NH2-RGFPRDPSTESG-COOH) in this study. Sections were dewaxed in xylene and rehydrated through graded ethanol series and, subsequently, incubated in 10% citrate buffer (pH 6.0) for 40 min in a 98°C water bath, for antigen retrieval. Endogenous peroxidase activity was quenched with 1% H_2O_2 and 100% methanol for 20 min. To prevent non-specific background staining, sections are incubated with Protein Block Serum-Free (Dako corporation) for 10 min at room temperature. Then, sections were incubated overnight with primary antibody at 4°C

and, subsequently, treated with the labeled polymer prepared by combining amino acid polymers with peroxidase and anti-rabbit polyclonal antibody (Histofine Simple Stain MAX PO MULTI, Nichirei). Peroxidase activities were visualized by diaminobenzidine staining, and the nuclei were stained with hematoxylin.

Disclosure of Potential Conflicts of Interest

No potential conflicts of interest were disclosed.

Acknowledgments

This work was supported by Grants-in-Aid for Scientific Research (A) (22249010) and Research (B) (21028026) from the Japan Society for the Promotion of Science (JSPS), by Grants-in-Aid for Scientific Research on Innovative Areas (22132004-A04) from the Ministry of Education, Culture, Sports, Science and Technology (MEXT), by Grants for Research on Intractable Diseases (H22–161) from the Ministry of Health, Labor and Welfare (MHLW), by Grant for National Center for Child Health and Development (23A-1), and by Grant from Takeda Science Foundation and from Novartis Foundation.

Supplemental Materials

Supplemental materials may be found here:
www.landesbioscience.com/journals/epigenetics/article/21937

References

1. da Rocha ST, Edwards CA, Ito M, Ogata T, Ferguson-Smith AC. Genomic imprinting at the mammalian Dlk1-Dio3 domain. Trends Genet 2008; 24:306-16; PMID:18471925; http://dx.doi.org/10.1016/j.tig.2008.03.011.
2. Kagami M, Sekita Y, Nishimura G, Irie M, Kato F, Okada M, et al. Deletions and epimutations affecting the human 14q32.2 imprinted region in individuals with paternal and maternal upd(14)-like phenotypes. Nat Genet 2008; 40:237-42; PMID:18176563; http://dx.doi.org/10.1038/ng.2007.56.
3. Kagami M, O'Sullivan MJ, Green AJ, Watabe Y, Arisaka O, Masawa N, et al. The IG-DMR and the MEG3-DMR at human chromosome 14q32.2: hierarchical interaction and distinct functional properties as imprinting control centers. PLoS Genet 2010; 6:e1000992; PMID:20585555; http://dx.doi.org/10.1371/journal.pgen.1000992.
4. Kagami M, Yamazawa K, Matsubara K, Matsuo N, Ogata T. Placentomegaly in paternal uniparental disomy for human chromosome 14. Placenta 2008; 29:760-1; PMID:18619672; http://dx.doi.org/10.1016/j.placenta.2008.06.001.
5. Lin SP, Youngson N, Takada S, Seitz H, Reik W, Paulsen M, et al. Asymmetric regulation of imprinting on the maternal and paternal chromosomes at the Dlk1-Gtl2 imprinted cluster on mouse chromosome 12. Nat Genet 2003; 35:97-102; PMID:12937418; http://dx.doi.org/10.1038/ng1233.
6. Sekita Y, Wagatsuma H, Nakamura K, Ono R, Kagami M, Wakisaka N, et al. Role of retrotransposon-derived imprinted gene, Rtl1, in the feto-maternal interface of mouse placenta. Nat Genet 2008; 40:243-8; PMID:18176565; http://dx.doi.org/10.1038/ng.2007.51.
7. Lage JM. Placentomegaly with massive hydrops of placental stem villi, diploid DNA content, and fetal omphaloceles: possible association with Beckwith-Wiedemann syndrome. Hum Pathol 1991; 22:591-7; PMID:1864589; http://dx.doi.org/10.1016/0046-8177(91)90237-J.
8. Yamazawa K, Kagami M, Nagai T, Kondoh T, Onigata K, Maeyama K, et al. Molecular and clinical findings and their correlations in Silver-Russell syndrome: implications for a positive role of IGF2 in growth determination and differential imprinting regulation of the IGF2-H19 domain in bodies and placentas. J Mol Med (Berl) 2008; 86:1171-81; PMID:18607558; http://dx.doi.org/10.1007/s00109-008-0377-4.
9. Georgiades P, Watkins M, Burton GJ, Ferguson-Smith AC. Roles for genomic imprinting and the zygotic genome in placental development. Proc Natl Acad Sci U S A 2001; 98:4522-7; PMID:11274372; http://dx.doi.org/10.1073/pnas.081540898.
10. Fowden AL, Sibley C, Reik W, Constancia M. Imprinted genes, placental development and fetal growth. Horm Res 2006; 65(Suppl 3):50-8; PMID:16612114; http://dx.doi.org/10.1159/000091506.
11. Georgiades P, Ferguson-Smith AC, Burton GJ. Comparative developmental anatomy of the murine and human definitive placentae. Placenta 2002; 23:3-19; PMID:11869088; http://dx.doi.org/10.1053/plac.2001.0738.
12. Tsai CE, Lin SP, Ito M, Takagi N, Takada S, Ferguson-Smith AC. Genomic imprinting contributes to thyroid hormone metabolism in the mouse embryo. Curr Biol 2002; 12:1221-6; PMID:12176332; http://dx.doi.org/10.1016/S0960-9822(02)00951-X.
13. Yamanaka M, Ishikawa H, Saito K, Maruyama Y, Ozawa K, Shibasaki J, et al. Prenatal findings of paternal uniparental disomy 14: report of four patients. Am J Med Genet A 2010; 152A:789-91; PMID:20186803; http://dx.doi.org/10.1002/ajmg.a.33247.
14. Suzumori N, Ogata T, Mizutani E, Hattori Y, Matsubara K, Kagami M, et al. Prenatal findings of paternal uniparental disomy 14: Delineation of further patient. Am J Med Genet A 2010; 152A:3189-92; PMID:21108407; http://dx.doi.org/10.1002/ajmg.a.33719.
15. Kagami M, Kato F, Matsubara K, Sato T, Nishimura G, Ogata T. Relative frequency of underlying genetic causes for the development of UPD(14)pat-like phenotype. Eur J Hum Genet 2012; 20:928-32; PMID:22353941; http://dx.doi.org/10.1038/ejhg.2012.26.
16. Seitz H, Youngson N, Lin SP, Dalbert S, Paulsen M, Bachellerie JP, et al. Imprinted microRNA genes transcribed antisense to a reciprocally imprinted retrotransposon-like gene. Nat Genet 2003; 34:261-2; PMID:12796779; http://dx.doi.org/10.1038/ng1171.
17. Davis E, Caiment F, Tordoir X, Cavaillé J, Ferguson-Smith A, Cockett N, et al. RNAi-mediated allelic trans-interaction at the imprinted Rtl1/Peg11 locus. Curr Biol 2005; 15:743-9; PMID:15854907; http://dx.doi.org/10.1016/j.cub.2005.02.060.
18. Köhrle J. Thyroid hormone transporters in health and disease: advances in thyroid hormone deiodination. Best Pract Res Clin Endocrinol Metab 2007; 21:173-91; PMID:17574002; http://dx.doi.org/10.1016/j.beem.2007.04.001.
19. Kraus FT, Redline RW, Gersell DJ, Nelson DM, Dicker JM. Disorders of placental Development. Placental Pathology (Atlas of Noutumor Pathology). Washington, DC: American Registry of Pathology, 2004:59-68.
20. Fox HE, Sebire NJ. The placenta in abnormalities and disorders of the fetus. Pathology of the Placenta. Third edition, Philadelphia, PA: SAUNDERS, 2007:262-3.
21. Parveen Z, Tongson-Ignacio JE, Fraser CR, Killeen JL, Thompson KS. Placental mesenchymal dysplasia. Arch Pathol Lab Med 2007; 131:131-7; PMID:17227114.
22. Nakayama M. Placental pathology. Tokyo, Igaku Shoin, 2002:106-7 (in Japanese).

厚生労働科学研究費補助金（成育疾患克服等次世代育成基盤研究事業）
分担研究報告書

分担課題：ARTの遺伝的安全性の検証

研究分担者　秦健一郎

研究要旨

近年、生殖補助医療技術、特に胚培養が、胚あるいは出生仔の遺伝子発現に影響を与えることがモデル生物で示され、注目されている。ヒトでは、生殖補助医療により出生した児で、エピジェネティックな異常が自然妊娠より高頻度に観察される可能性を懸念する症例報告がなされている。そこで、発生異常により淘汰されないと予想されるゲノム領域のDNAメチル化状態の「ゆらぎ」を、生殖補助医療により出生した児で解析する体制を構築し、試験的検証を行った。エピジェネティックな異常を検出・判定するためには、一般健常集団を含めたDNAメチル化状態の「ばらつき」に関する正確な知見と統計解析が必須であった。

A. 研究目的

体外受精などの生殖補助医療技術が胚発生に与える影響が、様々な観点から検証されている。近年、生殖補助医療技術、特に胚培養が、胚あるいは出生仔の遺伝子発現に影響を与えることがモデル生物で示され、注目されている。ヒトでは、生殖補助医療により出生した児で、ゲノムインプリンティング異常が自然妊娠より高頻度に観察される可能性を懸念する症例報告がなされている。胚の遺伝子発現に影響を与える分子機構として、エピジェネティックな遺伝子発現制御が有力な候補として示唆されているが、ヒトで網羅的系統的に解析した例は無い。そこで、ヒトART出生児のDNAメチル化状態を、特定領域（胎児胎盤の発生に重篤な影響を与える領域）に限定せず、広範に検証することで、発生異常により淘汰されないDNAメチル化異常を検出する機会が増える事を期待し、網羅的なDNAメチル化解析を行い、統計的な差異の有無を検証する。

B. 研究方法

妊娠36週以降に出生した新生児のうち、母体年齢を一致させたART群10-20例と、コントロール群10-20例の臍帯血ゲノムDNAを用い、Infinium Human Methylation450Beadchipで、常染色体上の42万か所のCpGサイトのDNAメチル化状態を比較検討する。

統計的な比較検討手法として、ART群とコントロール群の網羅的DNAメチル化データのクラスター解析を行う。事前情報無しに両群のゲノムワイドなDNAメチル化状態をクラスター解析することで、軽微な変化のため見過ごされている「隠されたDNAメチル化変化」の有無を検証する。また、各プローブのシグナル値（DNAメチル化状態）のばらつきを群間比較し、「DNAメチル化の揺らぎ」がART群で大きくなる可能性を検証する。

倫理面への配慮

本研究の遂行にあたっては、ヒトゲノム・遺伝子研究に関する倫理指針、疫学研究に関する倫理指針を遵守する。本研究に関わる症例検体収集及び解析の詳細は、国立成育医療研究センター倫理委員会の承認を受けた（承認番号234、406）